IMPACT OF RAPID ACCELERATION ON BEAM DYNAMICS IN THE RAPID-CYCLING SYNCHROTRONS OF A MUON COLLIDER *

L. Soubirou[†,1], A. Chance[‡,1], D. Amorim[2], H. Damerau[3], E. Lamb[3], E. Metral[3], L. Thiele[3,4]
[1]Université Paris-Saclay - CEA, France
[2]École Polytechnique Fédérale de Lausanne, Lausanne, Switzerland
[3]CERN, Geneva, Switzerland
[4]University of Rostock, Rostock, Germany

Abstract

Circular muon colliders offer a promising route to multi-TeV center-of-mass energies with high luminosity. The baseline design for the high-energy complex includes a chain of pulsed synchrotrons covering energies from 63 GeV to 5 TeV. This chain combines normal and hybrid synchrotrons, using both fixed-field superconducting and pulsed normal-conducting magnets. The short muon lifetime (2.2 µs in the rest frame) constitutes a major challenge for the accelerator complex: attaining high luminosity requires a muon survival rate of up to 70 % throughout the acceleration chain, which implies acceleration within a few milliseconds. Such rapid acceleration causes a mismatch between the beam energy in the arcs and the linearly ramped fields of the dipoles and quadrupoles. The corresponding field errors affect both the beam trajectory and optical functions. Preliminary tracking studies have been conducted to assess the emittance growth arising from these effects.

INTRODUCTION

Circular muon colliders provide a promising path to reach multi-TeV centre-of-mass energies with high luminosity. A baseline design for a muon collider was developed by the US Muon Accelerator Program (MAP) [1]. Within the framework of the International Muon Collider Collaboration (IMCC) and the MuCol program, an updated design is currently under investigation [2]. After production, the muon beam is cooled to reduce its transverse and longitudinal emittance. It is then accelerated to 63 GeV, using a linear accelerator followed by two recirculating linacs. Subsequently, a chain of Rapid-Cycling Synchrotrons (RCS) accelerates the beam to collision energy. Finally, the muons are injected into the collider ring. The layout of the muon collider is presented in Fig. 1.

The fast decay of the muon beam (with a lifetime of 2.2 µs in the rest frame) represents the principal challenge for the muon collider facility, since production, cooling, acceleration, and collision must all occur within the relativistically dilated muon lifetime. Reaching high luminosity requires a total survival rate of up to 70 % throughout the acceleration chain, which demands for acceleration through the entire chain of RCS in about ten milliseconds. Four RCSs accelerate the beam from 63 GeV to 5 TeV with energy stages at 314 GeV, 750 GeV and 1.5 TeV. The first RCS is a conventional synchrotron, whereas the following are hybrid RCS. The hybrid RCS consists of fixed-field superconducting dipoles interleaved with normal-conducting dipoles that pulse from negative to positive saturation. These pulsed dipoles provide rapid cycling and fast acceleration, while fixed-field strong dipoles help achieve a high average bending field for a compact ring. Due to the extremely fast acceleration, the pulsed magnets must be ramped at rates of up to 4.2 kT/s for RCS1. Such ramps create a mismatch between the discretely increased beam energy and the continuously ramped fields of the pulsed magnets, which include dipoles and quadrupoles. For RCS1, with a distribution of radiofrequency (RF) cavities over 8 stations, it represents a dipolar error of up to 3 % in the first arc. The consequences of this error on the beam dynamics are carefully studied for RCS1, the accelerator with the fastest acceleration of the chain. The first RCS of the chain covers an energy range from 63 GeV to 314 GeV in 0.34 ms. The beam circulates for 17 turns in a 5990 m long ring, providing an energy gain of 14.8 GeV per turn. A lattice design with 8 arcs is considered, featuring 90° FODO cells and a dispersion suppressor at entrance and exit of the RF insertions. The transverse and longitudinal emittances, $\varepsilon_{x,y}$ and ε_s, are set at 25 µm and 0.025 eV s, respectively.

ANALYTICAL MODEL

We consider a dipole of length L with its entry face placed at s_0, with the reference $s = 0$ at the beginning of the arc. Following the ramp, the strength of an infinitesimal slice of dipole at s is a function of the longitudinal position along the arc:

$$k_0(s) = k_0^* + k_0' \, (s - s^*) \tag{1}$$

where k_0^* is the strength at the reference energy, s^* the position where the magnetic field crosses the reference field, $k_0' \equiv \dot{B}/(B\rho c)$, with $\dot{B}$ the dipole ramp, $(B\rho)$ the magnetic rigidity, and c the light velocity.

In the following 6D treatment, $M_{a\to b}$ and $T_{a\to b}$ denote the reference 1st order and 2nd order transfer matrices from $s = a$ to $s = b$. We define the element reference transport matrix as $M = M_{s_0 \to s_0 + L}$. The quantities $\delta X(s)$ and $\delta M(s)$

* Endorsed by the IMCC. Funded by the European Union (EU). Views and opinions expressed are however those of the author(s) only and do not necessarily reflect those of the EU or European Research Executive Agency (REA). Neither the EU nor the REA can be held responsible for them.
† lisa.soubirou@cea.fr
‡ antoine.chance@cea.fr

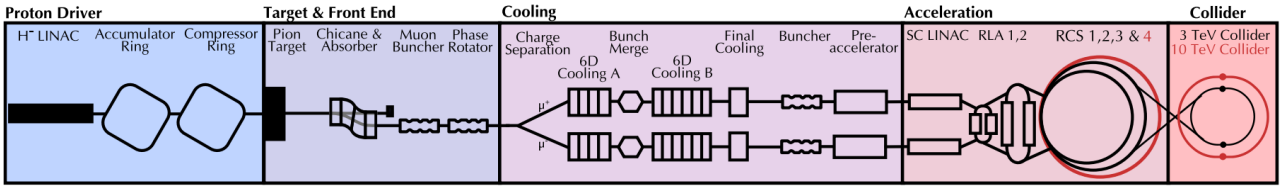

Figure 1: Muon collider facility layout [3].

denote the infinitesimal perturbations of the offset and 1st order matrix in s. Finally, ΔX and ΔM are the integrated offset and matrix perturbation of the element. We are looking to express the transport matrix of the pulsed dipole M_{pulsed} as

$$M_{\text{pulsed}} = M + \Delta M \tag{2}$$

The integrated offset and matrix perturbation of a pulsed dipole can be defined as

$$\Delta X(s_0) = \int_{s_0}^{s_0+L} M_{s\to s_0+L}\, \delta X(s)\, ds \tag{3}$$

$$\Delta M(s_0) = \int_{s_0}^{s_0+L} M_{s\to s_0+L}\, \delta M(s)\, M_{s_0\to s}\, ds + 2\int_{s_0}^{s_0+L} T_{s\to s_0+L}\big(M_{s_0\to s}, \delta X(s)\big)\, ds \tag{4}$$

The only non-null terms of $\delta X(s)$ and $\delta M(s)$ are

$$\delta X_2(s) = -k_0'(s - s^*) \tag{5}$$

$$\delta M_{2,1}(s) = -k_0^*\, k_0'(s - s^*) \tag{6}$$

The horizontal position offset created by this dipole, assuming $k_0^* L \ll 1$, is expressed as

$$\Delta X_1(s_0) \approx -\frac{1}{6}\, k_0'\, L^2\, (L + 3s_0 - 3s^*) \tag{7}$$

The horizontal offset is proportional to the dipole ramp rate but decreases with the magnetic rigidity of the beam.

A similar derivation can be made for a pulsed quadrupole. The quadrupole strength is of the same form as Eq. (1), but with $k_1' = \dot{G}/(B\rho c)$, with $\dot{G}$ the gradient ramp. A pulsed quadrupole does not generate any offset, $\delta X = 0$, and the only non-null terms of $\delta M_{\text{qd}}(s)$ are

$$\delta M_{\text{qd}\,2,1}(s) = -k_1'(s - s^*) \tag{8}$$

$$\delta M_{\text{qd}\,4,3}(s) = k_1'(s - s^*) \tag{9}$$

The results of the analytical model are implemented and compared with those obtained using the code Xsuite [4]. The analytical model provides transfer matrices that are inserted after each pulsed element as line elements. In parallel, each pulsed element is sliced and assigned a progressively increasing magnetic field to reproduce the ramp along the arc.

IMPACT ON THE TRAJECTORY AND OPTICS

The magnetic reference is chosen at the centre of the arc, $s^* = L_{\text{arc}}/2$. The ramped magnetic field, therefore, crosses the reference field at the middle of the arc, ensuring that the counter-rotating μ^+/μ^- beams experience a symmetric error.

The horizontal trajectory offset in the first arc of RCS1 is shown in Fig. 2, demonstrating excellent agreement between the analytical model and the sliced simulation. In the first half of the arc, the trajectory offset is positive because the magnetic field is weaker than the value corresponding to the reference beam energy. In the second half, the offset becomes negative as the magnetic field exceeds the reference field. The beam offset reaches a maximum of 13 mm. During acceleration in RCS1, the beam undergoes oscillations that are adiabatically damped as the beam energy increases, as Fig. 3 shows, confirming the energy dependence predicted by Eq. (7). The largest trajectory excursion, therefore, occurs when the beam passes through the first arcs of the ring.

Equation (7) also predicts a proportional dependence of the maximum trajectory excursion on the ramp speed. This behaviour is confirmed by performing a scan with acceleration times longer than the nominal value t_{acc}. The results are shown in Fig. 4.

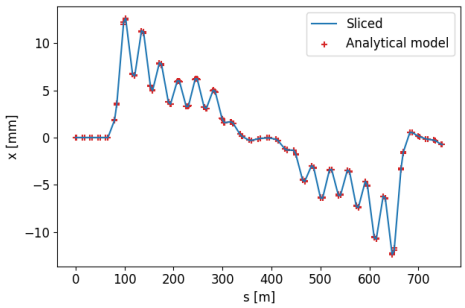

Figure 2: Horizontal trajectory offset in the first arc of RCS1.

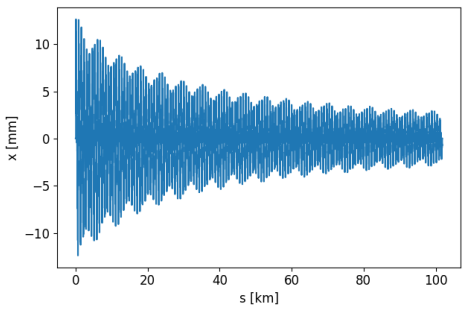

Figure 3: Horizontal trajectory offset for the entire acceleration in RCS1.

The impact on the optics is then studied in two configurations: first, considering the ramp only on the dipoles, and second, including both dipoles and quadrupoles. In both

scenarios displayed in Fig. 5, an error on the normalised dispersion is observed, reaching up to 0.1 $m^{1/2}$. When only pulsed dipoles are considered, the beta-beating remains moderate. However, when pulsed quadrupoles are included, it increases to as much as 20 % in both the horizontal and vertical planes. This represents a significant beta-beating, especially given that no other sources of errors are included in the model, such as misalignments, rolls, or mechanical vibrations. The perturbation of the optics exhibits the same dependence on the acceleration time, as shown in Fig. 4.

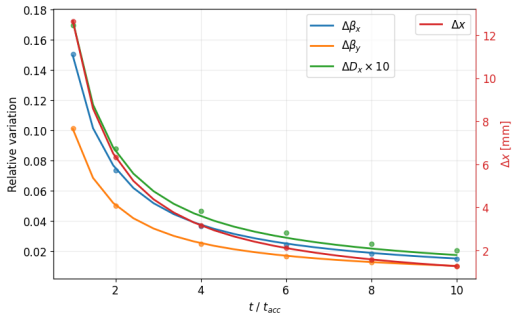

Figure 4: Maximum trajectory excursion and relative variation of optics as a function of the acceleration time.

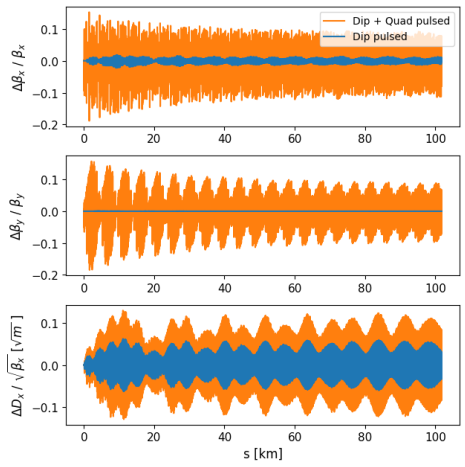

Figure 5: Perturbation on optics functions when dipoles (dip) and quadrupoles (quad) are pulsed for the entire acceleration in RCS1.

TRACKING STUDIES

Without considering the ramp in the pulsed elements, tracking studies performed on the lattice with 8 arcs and the nominal longitudinal emittance show a horizontal emittance growth exceeding 500 %, as presented in Fig. 6. When the longitudinal emittance is reduced by almost a factor 10, reaching 0.0026 eV s, the horizontal emittance growth decreases to only a few percents. Additionally, keeping the nominal longitudinal emittance while distributing the RF system across 28 stations rather than 8 eliminates the emittance growth.

Given that the lattices with 8 and 28 arcs have similar momentum compaction factors, 7.4×10^{-4} and 8.5×10^{-4}, and comparable horizontal chromaticities, −60.4 and −66.5, we attribute the observed emittance growth to the large energy spread of the beam (up to 4 %) combined with the strong energy kicks delivered by the RF cavities. These effects are transferred to the horizontal plane through synchro-betatron coupling. The potential contribution of second-order dispersion in the cavity still needs to be investigated.

In a second phase, we aim to quantify the emittance growth induced by the fast ramp. For the configuration with 8 arcs, tracking studies are performed with a longitudinal emittance of 0.0026 eV s. Despite this reduced longitudinal emittance, a horizontal emittance growth of up to 100 % is still observed. For the 28 arc lattice, using the nominal longitudinal emittance of 0.025 eV s, the horizontal emittance growth remains limited to about 10 %. These results strongly suggest that distributing the RF system over a larger number of sections is necessary to mitigate emittance growth induced by the fast ramp.

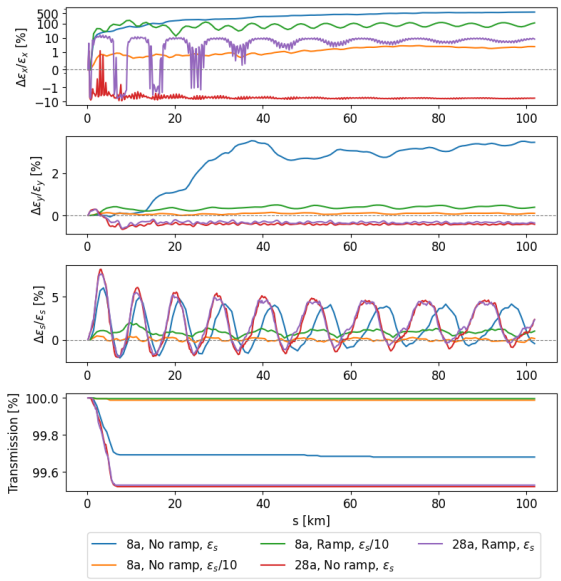

Figure 6: Start-to-end tracking results for RCS1 for lattices with 8 and 28 arcs, considering nominal and reduced longitudinal emittance and the fast ramp in the pulsed elements (ramp) or not (no ramp).

CONCLUSION

The impact of rapid acceleration is investigated for RCS1, the fastest ramping accelerator in the chain. An analytical model is developed and compared with simulation results to study the effects arising from the mismatch between the beam energy and the magnetic field of the pulsed elements. This mismatch leads to trajectory offsets and perturbs the optics, resulting in significant beta-beating. Even in the absence of ramp errors, tracking studies indicate that the RF system must be distributed over more than 8 stations to preserve the beam emittance. A lattice featuring 28 RF stations is found to limit the emittance growth to approximately 10 % when ramp errors are included.

REFERENCES

[1] MA. Palmer, "The US Muon Accelerator Program", in *Proc. 5th International Particle Accelerator Conference (IPAC'14), Dresden, Germany, June 15-20, 2014*, Dresden, Germany, pp. 1367–1369, Jul. 2014. doi:https://doi.org/10.18429/JACoW-IPAC2014-TUPME012

[2] C. Accettura *et al.*, "Interim report for the International Muon Collider Collaboration (IMCC)", 2025, arXiv: 2407.12450,

[3] R. Taylor *et al.*, "Consolidated parameters", *Consolidated Parameters*, 2025. doi:10.5281/ZENODO.17476875

[4] G. Iadarola *et al.*, "Xsuite: An Integrated Beam Physics Simulation Framework", in *Proc. 68th Adv. Beam Dyn. Workshop High-Intensity High-Brightness Hadron Beams (HB'23)*, Geneva, Switzerland, Oct. 2023, pp. 73–80. doi:https://doi.org/10.18429/JACoW-HB2023-TUA2I1